AGU
ADVANCING EARTH AND SPACE SCIENCE

Geophysical Research Letters®

Key Points:

- We report on two decades of earthshine measurements of the earth's reflectance made from Big Bear Solar Observatory yielding a large-scale terrestrial albedo
- We find a decline in albedo between 1998 and 2017, corresponding to a radiative increase of 0.5 W/m², which is climatologically significant
- The CERES data show the same behavior, which is attributed to a reversal of the Pacific Decadal Oscillation reducing the Earth's albedo

Correspondence to:

P. R. Goode,
pgoode@bbso.njit.edu

Earth's Albedo 1998–2017 as Measured From Earthshine

P. R. Goode[1] , E. Pallé[2,3] , A. Shoumko[1], S. Shoumko[1], P. Montañes-Rodriguez[2,3] , and S. E. Koonin[4]

[1]Big Bear Solar Observatory, New Jersey Institute of Technology, Big Bear, CA, USA, [2]Instituto de Astrofísica de Canarias (IAC), La Laguna, Spain, [3]Deptartamento de Astrofísica, Universidad de La Laguna (ULL), La Laguna, Spain, [4]Department of Physics, New York University, New York, NY, USA

Abstract The reflectance of the Earth is a fundamental climate parameter that we measured from Big Bear Solar Observatory between 1998 and 2017 by observing the earthshine using modern photometric techniques to precisely determine daily, monthly, seasonal, yearly and decadal changes in terrestrial albedo from earthshine. We find the inter-annual fluctuations in albedo to be global, while the large variations in albedo within individual nights and seasonal wanderings tend to average out over each year. We measure a gradual, but climatologically significant ~0.5 W/m^2 decline in the global albedo over the two decades of data. We found no correlation between the changes in the terrestrial albedo and measures of solar activity. The inter-annual pattern of earthshine fluctuations are in good agreement with those measured by CERES (data began in 2001) even though the satellite observations are sensitive to retroflected light while earthshine is sensitive to wide-angle reflectivity. The CERES decline is about twice that of earthshine.

Plain Language Summary The net sunlight reaching the Earth's climate system depends on the solar irradiance and the Earth's reflectance (albedo). We have observed earthshine from Big Bear Solar Observatory to measure the terrestrial albedo. For earthshine we measure the sunlight reflected from Earth to the dark part of the lunar face and back to the nighttime observer, yielding an instantaneous large-scale reflectance of the Earth. In these relative measurements, we also observe the sunlit, bright part of the lunar face. We report here reflectance data (monthly, seasonal and annual) covering two decades, 1998–2017. The albedo shows a decline corresponding to a net climate forcing of about 0.5 W/m^2. We find no correlation between measures of solar cycle variations and the albedo variations. The first precise satellite measures of terrestrial albedo came with CERES. CERES global albedo data (2001-) show a decrease in forcing that is about twice that of earthshine measurements. The evolutionary changes in albedo motivate continuing earthshine observations as a complement to absolute satellite measurements, especially since earthshine and CERES measurements are sensitive to distinctly different parts of the angular reflectivity. The recent drop in albedo is attributed to a warming of the eastern pacific, which is measured to reduce low-lying cloud cover and, thereby, the albedo.

1. Introduction

The Earth's albedo (or reflectance) is the fraction of shortwave solar radiation that it reflects back to space. It is an essential determinant of the earth's climate, since, in the broadest sense, changes in climate arise from the simultaneous evolution of the solar intensity, the Earth's albedo, and greenhouse insulation.

In the mid-1990's, the changing albedo was (and probably still is) the least understood of the three parameters (Houghton, 2000; IPCC, 2013). That uncertainty motivated our effort to measure of the earth's albedo continuously throughout at least one full solar cycle (two decades). The long data series would also help explore any correlations that might exist between varying solar activity and terrestrial reflectance (Gray et al., 2010; Haigh, 1996; Haigh et al., 2010; Lam & Tinsley, 2015; J. Lean et al., 1995; J. L. Lean, 2018; Svensmark, 1998).

The earthshine project began in Big Bear Solar Observatory (BBSO) in the mid-1990's to measure the Earth's albedo utilizing observations of the Moon as pioneered by Danjon (1928) nearly a century ago. Earthshine was first explained by Leonardo DaVinci (c. 1510), as sunlight reflected from the dayside Earth to the dark portion of the lunar disk as seen from the nighttime Earth. Our observations of the earthshine (or "ashen

light") were made from BBSO in California using modern photometric techniques. The globally integrated Earth's albedo measured using earthshine (Goode et al., 2001) is ~0.3 in the visible range.

This paper is a summary report of the BBSO Earthshine project. After irregular and randomly spaced trial observations in 1994–1995, sustained observations began in 1998 and ran through the end of 2017, acquiring about 1,500 nights of useable data over two decades. We report and interpret for the first time the totality of the monthly, annual, seasonal and decadal variations of the earth's albedo as derived from our earthshine measurements.

2. Earthshine Measurements of the Albedo
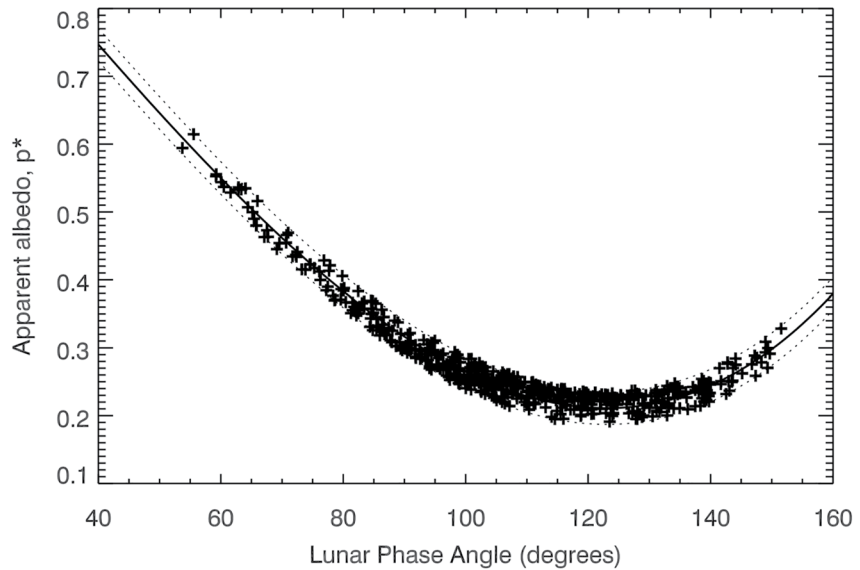
2.1. Earthshine Observations

Our earthshine observations during a waxing Moon are sensitive to the parts of the Earth west of Big Bear, across the Pacific to Asia and Australia, to the west of the Urals; they measure the reflectance of up to 40% of the Earth's surface in a single night. That large-scale reflectance can change by up to 10% in an hour, as when the sun rises over a cloudy Asia (Goode et al., 2001). During a waning Moon, we observe a portion of the Earth extending from west of Urals to the eastern part of North America, so including all of Africa and all of South America.

The variations of earthshine within a single day can be understood as resulting from changing terrestrial scenes. For example, the reflectivity of oceans is <10%, or about half that of land, while clouds reflect about half the sunlight, and snow/ice even more. Over a year, the reflectivity depends on seasons (because of Earth's north-south land asymmetry), snow/ice cover and cloud patterns. Both daily and seasonal variations in the Earth's albedo contribute to making it a challenging task to measure, say, an annual average terrestrial reflectance.

The first earthshine telescope used for regular observations between 1998 and 2007 is described in detail in Appendix A of Qiu et al. (2003). That refracting telescope had a Lyot stop to eliminate stray light and alternated observations of the bright (moonshine) and the dark (earthshine) regions of the Moon. Observations over 73 irregularly spaced nights during 1994–1995 were used to prove the concept while developing observing procedures and data analysis software. Regular observations began in December 1998 and continued through January 2007 with that earthshine telescope operating under the primary dome at BBSO.

In 2005, a small dome dedicated to earthshine work was constructed near the main dome and a new, smaller semi-automated earthshine telescope was constructed, installed, and tested (Goode et al., 2010). The two telescopes were run simultaneously for calibration purposes from September 2006 through January 2007. The clearest 10 nights during those five months covered a wide range of absolute lunar phase angles (70° - 140°) and showed an excellent agreement between variations in the reflectivity determined by the two instruments. However, there was a small constant offset (independent of lunar phase) between the two. After modeling both telescopes, we found the primary cause for that discrepancy was a slight difference in the wavelength coverage of the two cameras; differences in telescope design played an insignificant role. From September 2006 until the end of 2017 observations were made with the automated telescope under the small dome. There is a gap in the data between November 2005 and August 2006 due to major construction work of the BBSO main dome to accommodate the first facility class solar telescope built in the U.S. in a generation.

For about half the nights of each month, we can precisely measure the earthshine on the dark part of the lunar disk. During half of those nights the Moon is waxing from new to more than half full as the lunar phase ranges from about -150° to about -50°. The earthshine observations during those nights began shortly after sunset. For the waning phase (lunar phases progressing from 50° to 150°) during the other half of the nights, observations began after midnight and ended shortly before sunrise. Each night of observation yields a single apparent albedo covering up to ~40% of the Earth (Pallé et al., 2009). Further, during each night of a waxing (waning) Moon, we measure an apparent albedo for nearly the same area of the earth west (east) of BBSO. Thus, the Big Bear earthshine observations provide apparent albedos covering the same ~ 80% of the Earth. The nightly apparent albedos can be integrated over a month to obtain a measure of the Earth's shortwave Bond albedo.

Figure 1. Nightly earthshine measurements of the apparent albedo from Big Bear Solar Observatory earthshine covering 1998–2017 are plotted as a function of the absolute value of the lunar phase. The third order polynomial fit to all the data is indicated by a thick black line, and the dotted lines enveloping the data are the 1σ standard deviation around that mean.

## 2.2. Earthshine Data Analysis

The full methodology for determining albedo from earthshine is detailed in two lengthy papers, see Qiu et al. (2003) and Pallé et al. (2003), and analyses of the data up through 2014 were given in several papers (Pallé et al., 2004, 2009, 2016). Briefly, we observe the relative brightness of two fiducial regions (Crisium and Grimaldi) on opposing edges of the Moon, one being in the sunshine and the other in the earthshine, with the role of each switching depending on whether the Moon is waxing or waning. For a given night, following Qiu et al. (2003) and Pallé et al. (2003), the apparent albedo, p^* is determined as

$$p^*(\beta) = \frac{3}{2 f_L(\beta)} \frac{p_b f_b(\theta)}{p_a f_a(\theta_0)} \frac{I_a/T_a}{I_b/T_b} \frac{R_{em}^2}{R_e^2} \frac{R_{es}^2}{R_{ms}^2},$$ (1)

where p^* is the albedo of a Lambert (perfectly diffusing) sphere that would have the same instantaneous reflectivity as the true Earth at the same phase angle. f_L is the Earth's Lambert phase function and β is the Earth's phase angle (the angle between the sunlight that is incident on the Earth and then reflected to a fiducial region on the dark part of the lunar disk). $f_{a,b}$ are the empirically determined phase functions derived from all the data of the fiducial regions normalized to $f(0) = 1$ at perfect retroflection. θ is the lunar phase angle (the Moon's selenographic phase angle, which is the angle between the direction to the Sun from a lunar fiducial region and the nighttime observer at BBSO), θ_o is the small angle between the path of the Earth light striking the lunar fiducial region and the path of the nearly retroflected earthshine to the BBSO observer. $\dfrac{I_a/T_a}{I_b/T_a}$ is the ratio of the earthshine intensity (I) to the moonshine intensity in the two opposing fiducial patches, after each is corrected by the observed atmospheric transmission (T) or airmass, and $\dfrac{p_b}{p_a}$ is the known ratio between the geometrical reflectivity of the two opposing fiducial patches. R_{em}, R_{es}, R_{ms} and R_e refer to the Earth-Moon distance, the Earth-Sun distance, the Moon-Sun distance and the Earth's radius, respectively. In terms of the Moon's phase angle, the Earth's phase angle, β, is given by $\beta \approx \pi - \theta$.

In Figure 1, we plot the apparent albedos for our entire data series, with positive and negative lunar phase angles bundled together and plotted with the thick solid line being a third degree polynomial fit has the form ($p^* = 1.157 - 0.0096\theta - 3.084 x 10^{-5}\theta^2 + 3.79 x 10^{-7}\theta^3$, where θ is the lunar phase angle) against the absolute value of the lunar phase angle. The dashed lines in the figure represent the 1σ standard deviation of the mean bounds. To construct this plot, we followed Palle et al. (2016) in which nights with larger error
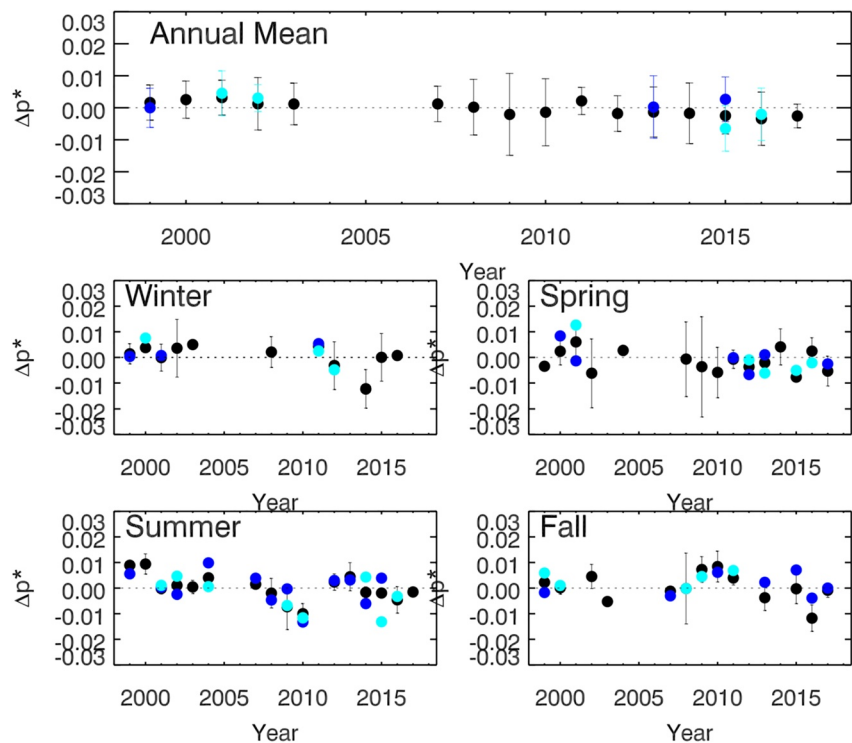
Figure 2. Mean annual and seasonal albedo trends, 1998–2017, from earthshine observations from Big Bear Solar Observatory. Black points represent the annual (top panel) and seasonal (lower four panels) average albedo deviation from the mean. The blue and cyan points represent annual and seasonal data from the positive (east-looking) and negative (west-looking) lunar phases, respectively.

with respect to the mean are iteratively eliminated. The essential effect of this clipping is to reduce the white noise in the data. Out of the 1529 nights originally with observations, only 801 are finally kept (53% of the total). The culled outlier nights typically correspond to very short observing nights and/or poor local weather conditions at BBSO. The larger magnitude phase angles correspond to a "near-crescent" Moon for which the gibbous Earth is nearly Lambertian and the apparent albedo is roughly comparable to the Earth's visible light Bond albedo (~0.3). The choice of 1σ for the clipping is somewhat arbitrary, but the result shown here are insensitive to modest variations in the choice of bandwidth of σ-clipping.

3. Results

3.1. Seasonal and Inter-Annual Trends in the Earthshine

Figure 2 displays earthshine results for two large, distinct, regions of the Earth: positive lunar phases sensitive to regions east of BBSO and negative lunar phases sensitive to regions west of BBSO. The black dots in the top panel are the annual mean albedo anomalies determined from the nineteen years of earthshine data in Figure 1 in which data are sorted into months and each month that has >5 nights with good observations that survived the culling process contributes to the anomaly for its year. The annual means are shown only for years in which at least each of six months of that year have at least five nights of data from Figure 1. Thus, there are more anomalies shown for some years/seasons than others. Further, in 2004–2006 too many nights were lost to telescope construction in Big Bear.

The blue and cyan points in the top panel show the annual means decomposed into their east and west components, respectively, while the lower four panels show the seasonal decomposition of the nineteen years of albedo anomalies. For each of the five panels, the yearly means are shown separately for the positive and negative phases, as well are for all phases. In all panels the seasonal anomalies are in good agreement among themselves and show similar patterns of inter-annual variability. The fact that the individual annual mean anomalies of positive and negative lunar phases agree well with the combined annual means, and that the

seasonal variations also seem to vary together, leads us to infer that the detected long-term fluctuations are global. Thus, we have binned the east and west regions together in our analyses. We note that he long-term variability is of the annual anomalies quite muted, with a long-term decline dominating the time series.

Among the seasonal averages, Summer and Fall have the largest inter-annual variability, of the order of $\Delta p^* \sim 0.01$, which is we matched for positive and negative phases. Spring is more muted but with more dispersion between the two time series. The Winter seasonal means stem from fewer observations due to seasonally poorer observing conditions in BBSO, which did not always allow collection of enough data to fully construct the desired times series.

3.2. Sun-Earth Relationships

Solar irradiance has been precisely measured from space for four decades. The Sun is, on average $\sim 0.1\%$ more irradiant at an activity maximum than at a minimum of its roughly 11 year activity cycle (Kopp & Lean, 2011). On the face of it, these cyclic changes in irradiance and activity are too small and short lived to do more than leave a weak signature in the climate (J. Lean et al., 1995; J. L. Lean, 2018; Gray et al., 2010). Perhaps the most famous of such Earth-Sun connections is the Maunder Minimum–coincident with the terrestrial "Little Ice Age," c.1645–1715 – when sunspots were rare (Eddy, 1976). Such connections have been hypothesized to occur through indirect, non-irradiant solar origins that alter the cloud cover in phase with the solar cycle (Haigh, 1996; Haigh et al., 2010; Lam & Tinsley, 2015; Svensmark, 1998).

Our period of observation (1998–2017) includes two solar maxima (2002 and 2014) with an intervening solar minimum (2009); solar minima conditions also occurred just before (1997) and just after (2019) the first and last years of observations. Our albedo measurements therefore cover nearly a full ~22 year solar cycle (full reversal and return of solar polar magnetic fields). Neither the globally averaged inter-annual variations nor the long-term trend in Earth's reflectance that we measure show a correlation with either the solar cycle (sunspot number), the cosmic ray flux, or any other solar activity indices. Our data, therefore, do not support an argument for any detectable imprint of direct or indirect solar activity mechanisms on the Earth's reflectance over the past two decades. One such indirect effect often mentioned is a cycle dependent seeding of cloud cover (Svensmark, 1998), hence changing albedo, as a result of cycle dependent shielding of galactic cosmic radiation. Rather, terrestrial phenomena that induce long-term changes in sea surface temperature (SST) or ice coverage (such as ENSO or multi-decadal oscillations) might well be the dominant drivers of the observed albedo changes. To probe this, we begin by comparing the earthshine and CERES albedo results.

3.3. Earthshine-CERES Comparison

The launch of the first CERES instruments in 2000 (Wielicki et al., 1996) began an era of high-quality terrestrial reflectance data that overlaps with most of our earthshine observations. From low-earth orbit, CERES measures the near retroflection of sunlight from individual small areas covering the Earth twice a day, and uses bi-directional reflectance models (Loeb et al., 2012) to infer the Bond albedo (light reflected in all directions). In that sense, earthshine observations, in which the sunlight is reflected from the earth at wide angles, are complementary to CERES observations of retroflected sunlight. The earthshine determination has the further advantage of being a relative measurement with simple instrumentation, therefore less prone to spurious long-term trends introduced by instrumental and calibration drifts.

For comparison with the Earthshine observations, we used the latest data set from the CERES instruments (Kato et al., 2018; Loeb, Doelling, et al., 2018), CERES-EBAF-TOA-Ed4.1 downloaded from the NASA LARC Ordering Tool (https://ceres-tool.larc.nasa.gov/). These data comprise the period from March 2003 to present. For earlier dates, the all-sky fluxes used here were derived from CERES Terra between 03/2000 to 06/2002 and CERES Terra + Aqua from 07/2002 onwards. While the data are available on a regional scale of 1° x 1°, we downloaded the globally averaged monthly means of the TOA Shortwave Flux (SW) flux, and the TOA Solar Flux variables (Doelling et al., 2016). The albedo is derived by the simple division of the SW flux by the solar flux. To compare with the earthshine measurements, we convert the albedo anomalies into W/m^2 units, by using the formula:
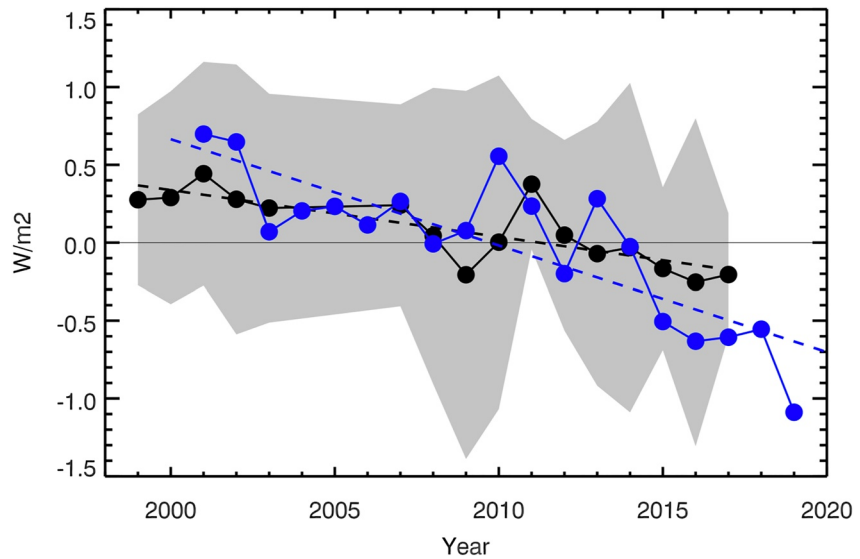
Figure 3. Earthshine annual mean albedo anomalies 1998–2017 expressed as reflected flux in W/m^2. The error bars are shown as a shaded gray area and the dashed black line shows a linear fit to the Earthshine annual reflected energy flux anomalies. The CERES annual albedo anomalies 2001–2019, also expressed in W/m^2, are shown in blue. A linear fit to the CERES data (2001–2019) is shown with a blue dashed line. Average error bars for CERES measurements are of the order of 0.2 W/m^2 .

$$\Delta E(t) = \Delta A(t)^* C(t) \tag{2}$$

where $C(t)$ is the TOA Solar flux and $\Delta A(t)$ are the albedo anomalies.

In Figure 3, we compare trends (in W/m^2) in annual Bond albedo anomalies from earthshine data (1998–2017) to CERES data (2001–2019). As mentioned, the earthshine nights selected come from the monthly anomalies in each year (but again, only months with >5 nights) so as to limit seasonal effects. The results are statistically the same if instead we had selected all the daily albedo anomalies from the years 1998–2003 and 2007–2017 from Figure 1 (not shown). The ground-based and satellite approaches make different assumptions beyond the data to determine the Bond albedo and its evolution. The CERES TOA short-wave reflected flux anomalies in the figure are derived from the retroflected satellite data plus modeled bi-directional reflectances (Loeb et al., 2012). For the earthshine, we determine the fractional annual effective albedo anomalies by calculating the average fraction, $\frac{\Delta p^*}{p^*}$, where each component of the average is the difference between a measured night in the year of interest and the overall fit to p^* for that phase angle as shown in Figure 1 (Goode et al., 2001; Pallé et al., 2003; Qiu et al., 2003). The connection to the Bond albedo anomalies would simply be $\frac{\Delta p^*}{p^*} = \frac{\Delta A}{A}$, and the changes in albedo are straightforwardly translated into changes in reflected energy flux at the TOA in W/m^2 multiplying the solar constant by one-quarter, $342\,W/m^2$.

CERES and Earthshine albedo observations have been compared before. Wielicki et al. (2005) found a strong anti-correlated behavior between the two time series over the period 2000 to 2003. However, the CERES data suffered at the time from an internal calibration drift; the full series was re-calibrated (Loeb et al., 2007). Palle et al. (2016) also compared CERES and earthshine trends during 2001–2014 and found a good general agreement. With the current datasets, it is striking how well the inter-annual earthshine anomalies agree with those from CERES, and that both show a downturn in the most recent years, even though they cover slightly different parts of the Earth. For the earthshine data, the albedo has decreased by about $0.5\,W/m^2$, and the decrease is significant (at the 5×10^{-5} level), while for CERES data, 2001–2017, the decrease of about 1.5 W/m^2 is significant at the level of 0.06. We note that the CERES data shows no trend after the first two years (2001 and 2002) until the sharp downturn beginning in 2015. These data were acquired from two different instruments, one on the Terra satellite launched in 2000 and the other on the Aqua satellite launched in mid-2002. From mid-2002 onward the data from both instruments were combined.

The CERES team has discarded the possibility of long-term calibration issues causing a drift in the data. Rather, they point to a recent appreciable increase in sea surface temperatures (SSTs) prominent off the west coasts of North and South America, which reduced the overlying low level cloud cover and consequently decreased the albedo (Loeb, Thorsen, et al., 2018). This is so since low clouds are highly reflective and because there is no cancellation between changes in short-wave (SW) and long-wave (LW) fluxes for low clouds, compared to other cloud types for which SW and LW effects are similar in magnitude but opposite in sign. Loeb, Thorsen, et al. (2018) attribute the SST warming to a flip in the Pacific Decadal Oscillation (PDO) from which the drop in albedo may signal the end of the 20 year hiatus in global warming. The flip began about 2014, peaked during the 2015–2017 period (last three years of earthshine data), and began to decline before the end of the decade. Thus, the story of whether or not the hiatus is ending likely will be told in the 2020s. For the last three years of earthshine data, CERES should (and does) see a larger decline than earthshine because earthshine is less sensitive to eastern Pacific coastal regions, which have the largest increase in SST. Nonetheless, we note that the earthshine is sensitive to the eastern Pacific off the west coast of North (South) America when the Moon is waxing (waning), so both positive and negative phase earthshine partially feel the effect of the PDO flip. Finally, we note that after the period of common earthshine and CERES data, there is an interesting and abrupt drop in CERES albedo in 2019.

4. Conclusions

We have reported a two-decade long data set of the Earth's nearly globally averaged albedo as derived from earthshine observations. Stringent data quality standards were applied to generate monthly and annual means. These vary significantly on monthly, annual, and decadal scales with the net being a gradual decline over the two decades, which accelerated in the most recent years. Remarkably, the inter-annual earthshine anomalies agree well with those from CERES satellite observations, despite their differences in global coverage, underlying assumptions to derive the albedo, and the very different sensitivities to retroflected and wider-angle reflected light.

The two-decade decrease in earthshine-derived albedo corresponds to an increase in radiative forcing of about 0.5 W/m^2, which is climatologically significant (Miller et al., 2014). For comparison, total anthropogenic forcing increased by about 0.6 W/m^2 over the same period. The CERES data show an even stronger trend of decreasing global albedo over the most recent years, which has been associated to changes in the PDO, SSTs and low cloud formation changes. It is unclear whether these changes arise from the climate's internal variability or are part of the feedback to external forcings.

As earthshine-derived global albedos are quite insensitive to long-term calibration issues (they are relative measurements), we hope that our results will encourage a resumption and revitalization of earthshine observations with new automated telescopes, DSCOVR-type observations, cubesat missions, or even a lunar observatory.

Data Availability Statement

The ASCII data file (date and albedo anomalies) used to create the figures here can be found at the BBSO website http://www.bbso.njit.edu/Data/Earthshine.txt.

References

Danjon, A. (1928). Revue des Travaux Astronomiques. *L'Astronomie*, *42*, 572–581.

Doelling, D. R., Sun, M., Nguyen, L. T., Nordeen, M. L., Haney, C. O., Keyes, D. F., & Mlynczak, P. E. (2016). Advances in geostationary-derived longwave fluxes for the CERES Synoptic (SYN1deg) product. *Journal of Atmospheric and Oceanic Technology*, *33*(3), 503–521. https://doi.org/10.1175/JTECH-D-15-0147.1

Eddy, J. A. (1976). The Maunder Minimum. *Science*, *192*(4245), 1189–1202. https://doi.org/10.1126/science.192.4245.1189

Goode, P. R., Qiu, J., Yurchyshyn, V., Hickey, J., Chu, M.-C., Kolbe, E., et al. (2001). Earthshine observations of the earth's reflectance. *Geophysical Research Letters*, *28*(9), 1671–1674. https://doi.org/10.1029/2000GL012580

Goode, P. R., Shoumko, S., Pallé, E., & Montañés-Rodríguez, P. (2010). Automated observations of the earthshine. *Advances in Astronomy*, *2010*, 963650. https://doi.org/10.1155/2010/963650

Gray, L. J., Beer, J., Geller, M., Haigh, J. D., Lockwood, M., Matthes, K., et al. (2010). Solar influences on climate. *Reviews of Geophysics*, *48*(4), RG4001. https://doi.org/10.1029/2009RG000282

Haigh, J. D. (1996). The impact of solar variability on climate. *Science*, *272*(5264), 981–984. https://doi.org/10.1126/science.272.5264.981

Haigh, J. D., Winning, A. R., Toumi, R., & Harder, J. W. (2010). An influence of solar spectral variations on radiative forcing of climate. *Nature*, *467*(7316), 696–699. https://doi.org/10.1038/nature09426

Houghton, J. T. (2000). The Solar Cycle And Terrestrial Climate, Solar And Space weather. In A. Wilson (Ed.), *IPCC report 2001* (Vol. 463, p. 255). Noordwijk, Netherlands: ESA Publications Division.

IPCC. (2013). *Climate change 2013: The physical science basis. Contribution of working group I to the fifth assessment report of the intergovernmental panel on climate change (Book)*, IPCC Report 2013. Cambridge, UK: Cambridge University Press. https://doi.org/10.1017/CBO9781107415324

Kato, S., Rose, F. G., Rutan, D. A., Thorsen, T. J., Loeb, N. G., Doelling, D. R., et al. (2018). Surface Irradiances of Edition 4.0 Clouds and the Earth's Radiant Energy System (CERES) Energy Balanced and Filled (EBAF) Data Product. *Journal of Climate*, *31*(11), 4501–4527. https://doi.org/10.1175/JCLI-D-17-0523.1

Kopp, G., & Lean, J. L. (2011). A new, lower value of total solar irradiance: Evidence and climate significance. *Geophysical Research Letters*, *38*(1), L01706. https://doi.org/10.1029/2010GL045777

Lam, M. M., & Tinsley, B. A. (2015). Solar wind-atmospheric electricity-cloud microphysics connections to weather and climate. *Journal of Atmospheric and Solar-Terrestrial Physics*, *149*(A12), 277–290. https://doi.org/10.1016/j.jastp.2015.10.019

Lean, J., Beer, J., & Bradley, R. (1995). Reconstruction of solar irradiance since 1610: Implications for climate change. *Geophysical Research Letters*, *22*(23), 3195–3198. https://doi.org/10.1029/95GL03093

Lean, J. L. (2018). Estimating solar irradiance since 850 CE. *Earth and Space Science*, *5*(4), 133–149. https://doi.org/10.1002/2017EA000357

Loeb, N. G., Doelling, D. R., Wang, H., Su, W., Nguyen, C., Corbett, J. G., et al. (2018). Clouds and the Earth's Radiant Energy System (CERES) Energy Balanced and Filled (EBAF) Top-of-Atmosphere (TOA) Edition-4.0 Data Product. *Journal of Climate*, *31*(2), 895–918. https://doi.org/10.1175/JCLI-D-17-0208.1

Loeb, N. G., Kato, S., Su, W., Wong, T., Rose, F. G., Doelling, D. R., et al. (2012). Advances in understanding top-of-atmosphere radiation variability from satellite observations. *Surveys in Geophysics*, *33*(1), 359–385. https://doi.org/10.1007/s10712-012-9175-1

Loeb, N. G., Thorsen, T. J., Norris, J. R., Wang, H., & Su, W. (2018). Changes in earth's energy budget during and after the "Pause" in global warming: An observational perspective. *Climate*, *6*(3), 62–80. https://doi.org/10.3390/cli6030062

Loeb, N. G., Wielicki, B. A., Rose, F. G., & Doelling, D. R. (2007). Variability in global top-of-atmosphere shortwave radiation between 2000 and 2005. *Geophysical Research Letters*, *34*(3), L03704. https://doi.org/10.1029/2006GL028196

Miller, R. L., Schmidt, G. A., Nazarenko, L. S., Tausnev, N., Bauer, S. E., Del Genio, A. D., et al. (2014). Cmip5 historical simulations (1850-2012) with giss modele2. *Journal of Advances in Modeling Earth Systems*, *6*(2), 441–478. https://doi.org/10.1002/2013MS000266

Pallé, E., Goode, P. R., & Montañés-Rodríguez, P. (2009). Interannual variations in Earth's reflectance 1999-2007. *Journal of Geophysical Research : Atmospheres*, *114*(9), D00D03. https://doi.org/10.1029/2008JD010734

Pallé, E., Goode, P. R., Montañés-Rodríguez, P., & Koonin, S. E. (2004). Changes in earth's reflectance over the past two decades. *Science*, *304*(5675), 1299–1301. https://doi.org/10.1126/science.1094070

Palle, E., Goode, P. R., Montañés-Rodríguez, P., Shumko, A., Gonzalez-Merino, B., Martinez-Lombilla, C., et al. (2016). Earth's albedo variations 1998-2014 as measured from ground-based earthshine observations. *Geophysical Research Letters*, *43*(9), 4531–4538. https://doi.org/10.1002/2016GL068025

Pallé, E., Goode, P. R., Yurchyshyn, V., Qiu, J., Hickey, J., Montañés Rodriguez, P., et al. (2003). Earthshine and the earth's albedo: 2. observations and simulations over 3 years. *Journal of Geophysical Research: Atmospheres*, *108*(D22), 4710. https://doi.org/10.1029/2003JD003611

Qiu, J., Goode, P. R., Pallé, E., Yurchyshyn, V., Hickey, J., Montañés Rodriguez, P., et al. (2003). Earthshine and the earth's albedo: 1. Earthshine observations and measurements of the lunar phase function for accurate measurements of the earth's bond albedo. *Journal of Geophysical Research: Atmospheres*, *108*(D22), 4709. https://doi.org/10.1029/2003JD003610

Svensmark, H. (1998). Influence of Cosmic Rays on Earth's Climate. *Physical Review Letters*, *81*(22), 5027–5030. https://doi.org/10.1103/PhysRevLett.81.5027

Wielicki, B. A., Barkstrom, B. R., Harrison, E. F., Lee, I., Robert, B., Smith, G. L., & Cooper, J. E. (1996). Clouds and the Earth's Radiant Energy System (CERES): An Earth Observing System Experiment. *Bulletin of the American Meteorological Society*, *77*(5), 853–868. https://doi.org/10.1175/1520-0477(1996)077<0853:CATERE>2.0.CO;2

Wielicki, B. A., Wong, T., Loeb, N., Minnis, P., Priestley, K., & Kandel, R. (2005). Changes in Earth's albedo measured by satellite. *Science*, *308*(5723), 825–825. https://doi.org/10.1126/science.1106484